JOURNAL INDIAN ASSOCIATION OF SEDIMENTOLOGISTS ISSN NO 2582 – 2020
Vol. 38, Issue 2, 2021, pp. 37-48
DOI: https://doi.org/10.51710/jias.v38i2.133

Lithofacies and petrochemical characterization of volcano-sedimentary sequence of Chandil Formation around Kharidih-Bareda area, Seraikela-Kharsawan District, Jharkhand: implications for uranium mineralization

Biswajit Panigrahi[1], S. P. Upadhyay[1], A. K. Sharma[1], Anirban Saha[1] and D. K. Sinha[2]
Atomic Minerals Directorate for Exploration and Research
[1]Jamshedpur [2]Hyderabad

Abstract

Mesoproterozoic Chandil Formation (ca. 1600 Ma) of North Singhbhum Mobile Belt record numerous features of felsic volcaniclastics and felsic to intermediate volcanics preserved in the central sector of the fold belt around Kharidih-Bareda area, Seraikela-Kharsawan district, Jharkhand. The felsic volcanic rocks exhibit flow bands, autoclasts and layering of crystal mushes revealing viscous nature of eruptives. The volcaniclastic sediments comprise of significant proportion of volcanic epiclasts and accidental lithic fragments. These volcaniclastics have been categorized into five prominent lithofacies viz, stratified lapilli tuff, banded tuff, tuff with penecontemporaneous deformation, welded lapilli stones, vitric tuff and volcanic bombs by field and petrographic studies of outcrops and subsurface borehole cores. The welded lapilli tuffs display fiamme and eutaxitic texture. Interlayering of the volcaniclastics, which are most often pyrite-rich, with psamo-pelitic lithology like carbonaceous phyllite, variegated phyllite, quartzite and minor limestone is suggestive of marine euxenic depositional environment.

Petrographic study of the volcaniclastics indicated presence of glass shards, garnet phenocrysts, spherules of tremolite, ovoid to lenticular accretionary lapilli along with devitrified glassy material. Compositionally these felsic volcanics and volcaniclastics are rhyodacitic to andesitic in nature with peraluminous to meta aluminous in character. A/CNK values vary from 0.52 to 2.42 in felsic volcanics and from 0.12 to 1.63 in volcaniclastics. Signatures of arc magmatism is indicated by low concentration of HFS elements such as Nb (5-17 ppm), Ga (11-17 ppm) and Y (5-28 ppm).

Elevated intrinsic content of uranium (3-8 ppm), Th/U ratio ranging from 1.2 to 13.2, presence of metamict allanite and zircon in volcanics and volcaniclastics reveal their suitability as a prospective source for search of uranium mineralization. The volcanic-volcaniclastic-clastic association of the Chandil Formation provides an ideal situation where provenance and province both are available. Thus, suitable litho-structural locales such as the concealed shear zones sympathetic to the Dalma thrust and South Purulia Shear Zone within the volcano-sedimentary package of Chandil Formation may be targeted as preferable sites for locating concealed uranium mineralization.

Key words: Lithofacies, felsic volcanics, uranium mineralization, Chandil Formation

Introduction:

The Paleo to Mesoproterozoic mobile belt delimited by Singhbhum Craton in the south and Chhotanagpur Granite Gneissic Complex in the north is known as North Singhbhum Mobile Belt (NSMB) or North Singhbhum Fold Belt (Gupta and Basu, 2000; Mahadevan, 2002). NSMB is longitudinally divided into two parts by a median spine shaped volcanic belt known as Dalma Volcanics (Fig. 1). The metasediments of NSMB exposed to the north of Dalma volcanics is known as Chandil Formation and is considered to be Mesoproterozoic (ca. 1600 Ma) in age (Ray et al., 1996; Sengupta et al., 2000; Mazumder, 2005; Reddy et al., 2009). Chandil

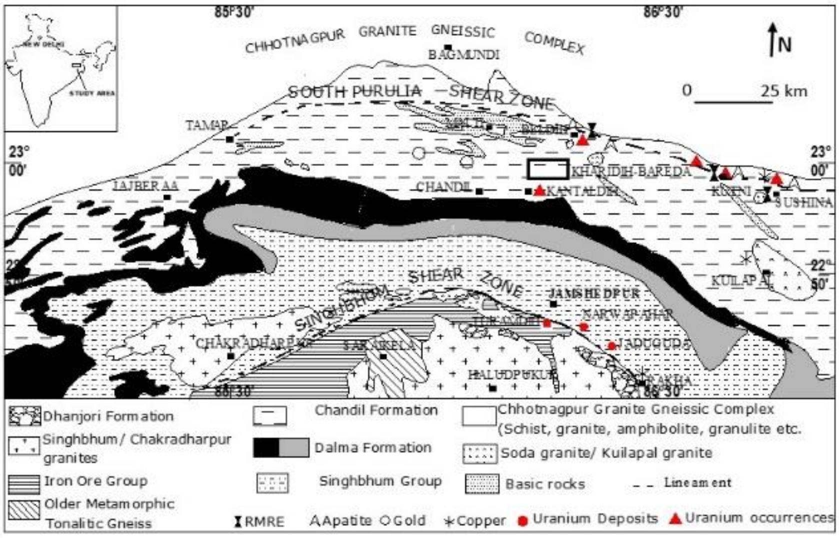

Fig. 1 Regional Geological map of North Singhbhum Mobile Belt showing location of the study area (Modified after Dunn and Dey, 1942; Mazumder, 2005)

Formation comprises lower green schist facies of rocks consisting of metapelites, metapsammites, basic intrusives and acid volcanics. Occurrences of acid volcanic rocks, viz, tuffs and rhyolites in this domain have been reported by several workers (Sengupta et. al., 2000). Isotopic data (Rb-Sr age 1484±44 Ma) of the acid volcanics of this belt suggests the presence of a Mesoproterozoic volcano-sedimentary basin in Singhbhum Craton (Sengupta et. al., 2000) which was subsequently upheld by various workers (Mazumder, 2005; Chatterjee et al., 2013; Mazumder et al., 2015). Geological and geochemical study of a part of these felsic volcanics and volcaniclastic units exposed along the South Purulia Shear Zone (SPSZ), occurring at the interface between Chandil Formation and Chhotanagpur Granite Gneissic Complex, has been described by Acharya et al. (2006). However, the information on the felsic volcanics and associated volcaniclastics still remains sparse and the data accrued are from a few selected localities. Detailed geological, lithofacies and geochemical characterization of rocks is lacking from many sectors of Chandil Formation.

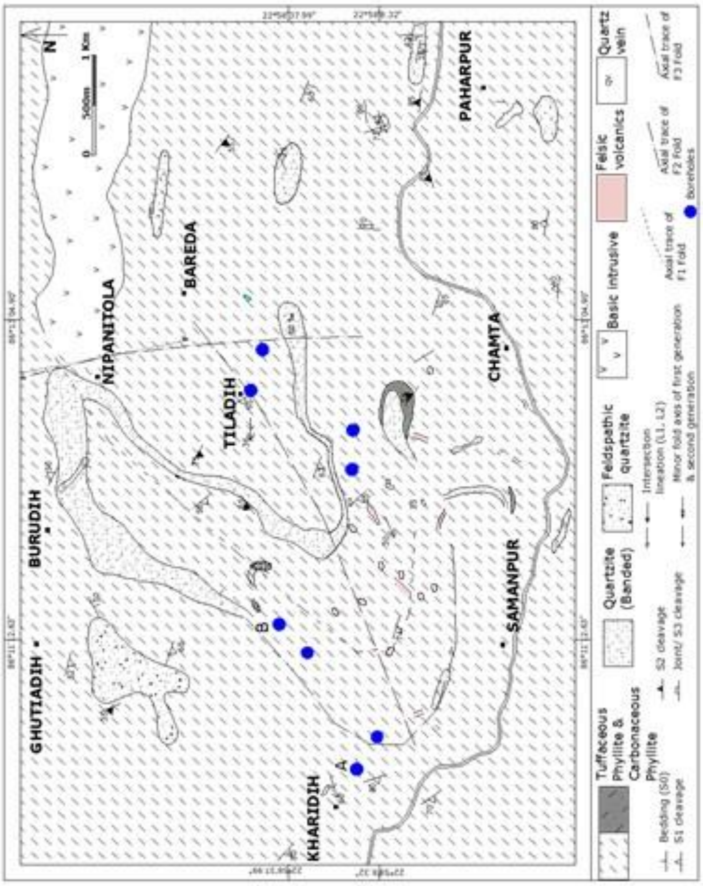

Fig. 2. Geological map of Kharidih Bareda area, Seraikela-Kharsawan District, Jharkhand showing complex outcrop pattern due to polyphase folding. Solid blue dots indicate the borehole locations where concealed felsic volcanics and volcaniclastics were recorded in subsurface. A and B represent the boreholes, the lithologs of which are shown in Fig. 12.

In the present study, the authors focus on characterization of different lithofacies of the felsic volcaniclastic and volcanic rocks exposed in the central sector of Chandil Formation, around Kharidh-Bareda, which lies about 15 km south of SPSZ and hitherto unstudied. Field, petrographic, geochemical and radiometric criteria have been utilized to characterize the rocks and highlight their potential as a suitable source as well as a host rock for uranium mineralization.

Geological Setting

The name Chandil Formation was given by Ray et al. (1996) to the lithopackage dominated by acid tuffaceous rocks exposed in the north of Dalma Volcanic belt. The tuffs were identified as vitric, lithic and crystal lithic tuffs (Ray et al.,1996). This meta-sedimentary belt is categorized under the northern most domain (domain V) of North Singhbhum Fold Belt by Gupta and Basu (2000). The general stratigraphy of the area is given in Table-1.

The Chandil Formation consists of meta-pelitic and psamo-pelitic sequence with felsic tuffs, acid volcanics, carbonaceous phyllite, minor interlayers of quartzite and occasional carbonate rocks showing low grade of metamorphism (Fig. 1). These are further intruded by younger basic sills and dykes.

Detailed mapping in the central sector of Chandil Formation, around Kharidih-Bareda, reveals tuffaceous phyllite covers a large part of the area (Fig. 2). These are variegated in nature with the colour varying from grey, light grey, buff to light greenish. Intercalations with bands of carbonaceous phyllite are observed in the south of Paharpur and Tilaidih. Two types of quartzite are exposed in the area. Fine grained, grey to dark grey coloured, banded quartzites are observed in the northern part, near Nipanitola and Burudih. These are cherty at places and intercalated with tuffaceous layers near Paharpur. Medium to coarse grained feldspathic quartzites showing intermittent silicification and ferugenisation are exposed in separate hillocks in the western part of the area around Ghutiadih.

Felsic volcanic are exposed as discontinuous bands within tuffaceous phyllite. These are massive, grey to dark grey in colour, fine grained, equigranular, hard, compact and form concordant lenses within the metasediments. An E-W trending amphibolite body extending over

Table 1 Generalized stratigraphy of Singhbhum Mobile Belt (Modified after Gupta and Basu, 2000 and Mazumder, 2005)

Age	Group	Formations	Lithology
Middle - Upper Proterozoic	Acidic - Alkaline rocks		Ultramafics, magnetite-apatite rocks
		Chandil Formation	Phyllite (±carbonaceous), tuff, felsic volcanic, quartzite
	Dalma Group	Upper Dalma Lower Dalma	Not represented
	Singhbhum Shear Zone Assemblage (>1.6 Ga)		
Lower Proterozoic	Singhbhum Group (>2.2 Ga)	Dalbhum	Quartzite, schist, phyllite
		Chaibasa	Medium grade Basic and pelitic schists
	Dhanjori Group (2.4 Ga)	Upper Dhanjori	Conglomerate., Quartzite, basic volcanics and schists
		Lower Dhanjori	
Archean	Cratonic basement		Older Metamorphic gneiss, Older Metamorphic Tonalitic Gneiss, Singhbhum Granite, Iron Ore Group and other granitoids

Fig. 3 Layering of crystal mushes in rhyodacitic flow shown between black dotted lines. Seen near Samanpur in Fig. 2

3.4km strike length with 600-900m width intrudes into these metasediments in the northeastern part. It is greenish black coloured, melanocratic, medium to fine grained and massive in nature. It has faulted contact with the metasediments in the west (Fig. 1).

The area has undergone three phases of folding. First generation of folds are tight, isoclinal and reclined in nature. These are refolded by second

Fig. 4 Flow bands of rhyodacitic rock observed in borehole at location A, shown in Fig. 2.

generation folds having ENE-WSW axial trend, which mostly controls the outcrop pattern. A major synformal closure of second generation having moderate plunge due SSW is identified near Kharidih in the western part. Broad open folds having near N-S axial trend define the third generation of folds. Fold interference has resulted in a complex outcrop pattern. Lateral discontinuity, polyphase folding and inadequate surface exposures are the hindrances in the mapping of individual volcaniclastic facies on a large-scale map.

VOLCANIC AND VOLCANICLASTIC ROCKS OF CHANDIL FORMATION

Felsic flows

Felsic flows are interlayered with argillites and volcaniclastic rocks. Interspersed outcrops occur intermittently in different parts of the area which is attributed to polyphase folding and peneplanation. These rocks are grey to dark grey coloured, fine grained, massive to crudely foliated in nature and break with a conchoidal fracture. Some of these exhibit development of mushes of feldspar crystals which impart crude layering to the rock (Fig. 3). Flow layers and bands are also discernible in borehole cores (Fig. 4).

Volcaniclastic rocks

The detailed mapping of the outcrops and

Fig. 5 Stratified lapilli tuff (Outcrop photo width 0.50m)

study of boreholes cores of key locations revealed different lithofacies of volcaniclastic rocks. On the basis of field relationship, petrographic studies, grain size, textural and structural features, the volcaniclastics have been classified into the following five facies: stratified lapilli tuff, banded tuff, welded lapilli stones, tuff with

Fig. 6 Stratified lapilli tuff horizon in borehole cores of location A in Fig. 2. Photo width 1m

penecontemporaneous deformation features and spheroidal volcanic bombs, arranged in decreasing order of preponderance. Non-mappable outcrops of individual facies preclude inference of any genetic

Fig.7 Outcrop photo showing foliation in welded lapilli stone

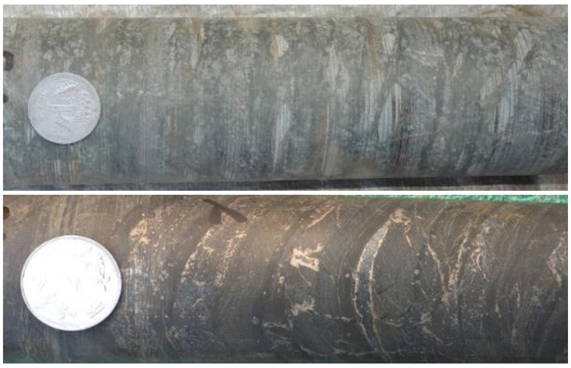

Fig. 8. Photographs of borehole cores at location B shown in Fig. 2. Top: Fiamme texture. Bottom: Pyrite encircles the lapilli clasts and also fills the cross fractures

connotation for these volcaniclastics. Thus, they are generalized under volcanic epiclasts and accidental lithoclasts. Grain size terminology used for classifying these volcaniclastics has been taken from Fischer (1966).

Stratified Lapilli Tuff

These facies comprise of predominantly tuffaceous material intermittently strewn with subangular to subrounded lapilli clasts. The size of the clasts varies from 3 mm to 5 cm (Fig. 5). Thick

Fig. 9 Banded tuff showing parallel lamination. Inset shows angular feldspar clasts set in argillaceous matrix

horizons ranging from 25m to 60m of this lithofacies have been recorded at several places in borehole columns. Stratification planes defined by tuffaceous and argillaceous layers are distinctly discernible giving the rock a layered appearance (Fig. 6).

Welded Lapilli stone

This facies is characterized by the distribution of lapilli of different sizes within the highly silicic matrix. The rock is very hard, compact

Fig. 10 Penecontemporaneous deformation feature in tuffaceous phyllite

and welded in appearance. Intermittent exposures of this facies are seen in the high lands in close proximity to the felsic to intermediate flows. The lapilli are lenticular in shape and strongly aligned along the plane of deformation (Fig. 7). Elongated lenses of lapilli clasts are compacted and strongly welded to define fiamme texture (Fig. 8).

Banded Tuff

Grey buff to light yellowish coloured, fine grained, thinly laminated rocks define this facies. It comprises abundant quartz and sericite with the

Fig. 11 Spheroidal to ellipsoidal shaped volcanic bombs bound by silicified matrix observed near Tilaidih area shown in Fig. 2

frequent distribution of wedge shaped glass shards. It has a distinct banded appearance (Fig. 9). A close examination of fresh and weathered surfaces reveals that the rock is constituted of coarse to fine sand sized subangular feldspar clasts set in argillaceous matrix. Sporadic exposures are best seen north of Chamta in the southeastern part and around Ghutiadih in the northwestern part of the studied area.

Tuff showing penecontemporaneous deformation

This facies occurs intermittently within the tuffaceous phyllites and lapilli tuff zone. These are exposed in the northern part of the area to the west of Nipanitola. It is characterised by 20-50 cm thick zone of convolute laminations and contorted bedding of coarser arenaceous layers within the tuffaceous phyllite (Fig. 10). Intraformational breccia zones recorded within the tuffaceous units in a few boreholes are also categorised under this facies. These features usually originate by palaeo seismicity events and can be attributed to volcanic activity in the study area.

Volcanic bomb

A few localized occurrences of welded bomb sized (> 64 mm) aggregates are observed as a plug like body, west of Tilaidih (Fig. 11). These silica rich clasts are spheroidal in nature and embedded in siliceous matrix. The bomb clasts are flattened due to deformation. Prima facie analogy with other lithotypes of the area suggests that the rocks may be juvenile fragments of semisolid magma ejected during eruptional activity.

Subsurface lithology observed in boreholes comprises of interlayering of stratified lapilli tuff, tuffaceous phyllite, psamopellitic rocks, rhyodacitic flow, welded lapilli stone, banded tuff and psamopelitic variants (Fig. 12). The shape of the lapilli varies from highly angular to subrounded. Chloritic bands along bedding and foliation planes as

Table 2 Major and trace element concentration of felsic volcanic rocks of Kharidih Bareda area

Samp	1	2	3	4	5	6	7	8	9	10	11	12	13	14	15	16
SiO_2	62.6	65.93	60.65	63.18	62.11	66.2	66.82	64.75	59.57	68.2	66.04	62.45	64.26	61.96	61.71	60.74
TiO_2	0.6	0.51	0.63	0.64	0.71	1.02	1.04	1.02	0.45	0.54	0.58	0.68	0.62	1.22	1.21	0.72
Al_2O_3	9.47	8.03	9.43	11.83	12.76	10.04	12.41	15.08	8.25	10.08	11.38	12.43	13.46	12.71	15.92	8.61
$Fe_2O_{3\,(T)}$	11.38	9.38	13.43	10.45	11.19	12.95	10.67	10.83	19.55	7.31	9.46	12.46	7.52	12.29	11.13	17.4
MgO	3.23	3.41	3.76	3.78	3.13	2.69	2.74	2.6	3.24	3.79	3.7	3.53	3.75	3.7	3.37	3.03
MnO	0.37	0.44	0.29	0.29	0.49	0.42	0.12	0.12	0.56	0.26	0.43	0.18	0.21	0.16	0.11	0.43
CaO	2.95	4.13	2.65	1.93	0.99	0.67	0.38	0.47	1.92	3.54	2.53	0.89	2.26	0.6	0.61	0.83
Na_2O	1.91	2.41	2.72	1.91	1.91	0.98	0.5	0.53	0.56	0.03	0.66	0.75	0.13	0.03	0.03	0.25
K_2O	4.51	3.65	4.8	5.95	5.9	4.17	4.51	5.41	3.59	4.08	4.32	4.74	6.12	4.42	4.99	4.78
P_2O_5	0.14	0.11	0.11	0.1	0.1	0.22	0.09	0.11	0.13	0.08	0.05	0.06	0.06	0.12	0.11	0.21
Total	97.16	98	98.47	100.06	99.29	99.36	99.28	100.92	97.82	97.91	99.15	98.17	98.39	97.21	99.19	97
A/CNK	0.71	0.52	0.65	0.90	1.13	1.37	1.94	1.99	0.99	0.92	1.10	1.56	1.23	2.15	2.43	1.21
A/NK	1.18	1.01	0.98	1.23	1.34	1.64	2.18	2.24	1.72	2.26	1.98	1.95	1.97	2.63	2.92	1.54
V	75	60	77	77	89	130	128	150	nd	59	63	88	64	157	171	nd
Cr	87	83	108	82	91	201	201	165	nd	62	79	127	57	199	204	nd
Co	36	30	40	33	36	48	41	37	nd	28	33	47	25	40	39	nd
Ni	32	33	25	31	37	49	60	61	nd	36	35	38	28	50	67	nd
Cu	<10	<10	<10	82	19	41	<10	<10	nd	12	11	<10	14	20	<10	nd
Zn	78	80	94	76	103	95	105	123	nd	82	70	115	78	41	58	nd
Ga	13	12	11	14	14	12	14	16	nd	13	13	13	15	14	16	nd
Rb	130	121	133	142	155	105	120	125	nd	126	116	111	183	99	131	nd
Sr	11	34	<10	21	<10	<10	11	11	nd	30	26	50	22	<10	10	nd
Y	13	5	16	16	21	16	15	17	-	5	5	5	25	5	28	nd
Zr	53	52	57	73	66	122	142	117	nd	85	83	74	95	191	154	nd
Nb	35	15	13	11	5	10	17	10	-	5	5	5	5	12	5	nd
Ba	1118	812	1220	1585	1257	479	523	840	nd	1014	1060	994	1152	574	708	nd
Ce	176	131	162	151	158	165	137	140	nd	84	121	138	94	150	160	nd
Pb	<10	<10	<10	<10	<10	<10	<10	13	nd	<10	21	33	<10	<10	<10	nd
Zr/SiO_2	0.011	0.009	0.010	0.009	0.011	0.009	0.012	0.014	0.011	nd	0.016	0.014	0.011	0.015	0.016	0.013

Analytical values of the major oxides are given % and trace element are given in ppm well as fracture planes of volcaniclastics are noteworthy. A significant amount of pyrite and minor chalcopyrite is associated with the lapilli-dominant sediments as well as the banded tuff (Fig. 8). Brownish to pinkish colour garnet are developed as specks and clots at many places suggesting that the metasediments have attained almandine facies metamorphism. Pyrite-bearing carbonaceous phyllite and intercalatory quartzite bands are also observed in some boreholes. Concealed bands of calcareous layers in the form of limestone and calcareous quartzite are noted in the boreholes drilled in the southwestern part of the area.

Table 3 Major and trace element concentration of volcaniclastic rocks of Kharidih Bareda area

Samp	18	19	20	21	22	23	24	25	26	27	28	29	30	31	32	33	34	35	36	37
SiO_2	67.79	61.29	60.95	62.65	58.19	48.64	47.05	53.8	56.79	44.81	49.93	49.15	54.51	53.96	55.66	58.83	55.35	58.54	52.5	47.7
TiO_2	0.69	0.47	0.52	0.71	0.43	0.52	0.43	0.55	0.66	0.18	0.42	0.24	0.36	0.33	0.62	0.56	0.53	0.4	0.39	0.55
Al_2O_3	11.29	8.7	10.06	11.86	7.87	7.08	5.26	6.17	10.1	0.88	4.1	1.96	3.64	5.41	8.75	11.93	10.98	7.34	7.68	10.19
$Fe_2O_{3\,(T)}$	6.98	14.92	16.34	11.06	17.97	27.15	26.49	23.75	19.27	31.57	26.73	28.28	24.44	26.49	20.67	15.45	18.78	19.31	24.61	23.64
MgO	2.18	3.5	3.1	3.34	3.96	4.11	4.38	3.68	3.24	2.38	3.82	3.74	2.98	4.04	4.46	3.09	3.92	3.99	4.5	5.14
MnO	0.06	0.28	0.21	0.5	0.27	0.91	0.76	1.89	0.5	0.63	0.96	1.12	1.37	0.67	0.49	0.15	0.48	0.57	0.58	0.2
CaO	0.81	2.89	0.97	1.37	2.85	2.48	3.97	1.97	0.82	3.13	2.96	6.63	3.77	3.41	3.19	0.71	0.96	2.38	2.32	1.14
Na_2O	3.26	0.03	0.87	3.37	1.01	1.35	0.91	0.72	1.09	0.27	0.6	0.38	0.57	0.56	3.49	0.55	0.97	0.96	0.9	2.16
K_2O	7.47	3.87	3.72	5.59	3.22	4.34	3.56	3.11	5.3	0.95	2.6	1.59	2.16	2.27	0.39	4.71	4.83	3.92	3.8	0.91
P_2O_5	0.08	0.1	0.1	0.1	0.14	0.21	0.21	0.89	0.2	0.15	0.43	0.31	1.36	0.17	0.17	0.09	0.16	0.19	0.29	0.24
Total	100.61	96.05	96.84	100.55	95.91	96.79	93.02	96.53	97.97	84.95	92.55	93.4	95.16	97.31	97.89	96.07	96.96	97.6	97.57	91.87
A/CNK	0.76	0.92	1.39	0.84	0.76	0.62	0.42	0.76	1.12	0.12	0.45	0.14	0.36	0.56	0.73	1.64	1.28	0.72	0.78	1.54
A/NK	0.84	2.05	1.84	1.02	1.53	1.02	0.98	1.36	1.34	0.60	1.08	0.84	1.11	1.60	1.42	1.99	1.61	1.26	1.37	2.25
V	102	nd	nd	82	nd	nd	nd	nd	nd	nd	nd	nd	nd	nd	nd	nd	nd	nd	nd	nd
Cr	121	nd	nd	93	nd	nd	nd	nd	nd	nd	nd	nd	nd	nd	nd	nd	nd	nd	nd	nd
Co	32	nd	nd	34	nd	nd	nd	nd	nd	nd	nd	nd	nd	nd	nd	nd	nd	nd	nd	nd
Ni	74	nd	nd	35	nd	nd	nd	nd	nd	nd	nd	nd	nd	nd	nd	nd	nd	nd	nd	nd
Cu	10	nd	nd	<10	nd	nd	nd	nd	nd	nd	nd	nd	nd	nd	nd	nd	nd	nd	nd	nd
Zn	19	nd	nd	40	nd	nd	nd	nd	nd	nd	nd	nd	nd	nd	nd	nd	nd	nd	nd	nd
Ga	14	nd	nd	13	nd	nd	nd	nd	nd	nd	nd	nd	nd	nd	nd	nd	nd	nd	nd	nd
Rb	168	nd	nd	127	nd	nd	nd	nd	nd	nd	nd	nd	nd	nd	nd	nd	nd	nd	nd	nd
Sr	13	nd	nd	25	nd	nd	nd	nd	nd	nd	nd	nd	nd	nd	nd	nd	nd	nd	nd	nd
Y	17	nd	nd	14	nd	nd	nd	nd	nd	nd	nd	nd	nd	nd	nd	nd	nd	nd	nd	nd
Zr	105	nd	nd	75	nd	nd	nd	nd	nd	nd	nd	nd	nd	nd	nd	nd	nd	nd	nd	nd
Nb	5	nd	nd	13	nd	nd	nd	nd	nd	nd	nd	nd	nd	nd	nd	nd	nd	nd	nd	nd
Ba	585	nd	nd	1258	nd	nd	nd	nd	nd	nd	nd	nd	nd	nd	nd	nd	nd	nd	nd	nd
Ce	65	nd	nd	150	nd	nd	nd	nd	nd	nd	nd	nd	nd	nd	nd	nd	nd	nd	nd	nd
Pb	<10	nd	nd	<10	nd	nd	nd	nd	nd	nd	nd	nd	nd	nd	nd	nd	nd	nd	nd	nd

Analytical values of the major oxides are given % and that of trace element are given in ppm
Nd: Not determined by XRF due to presence of higher content of Fe

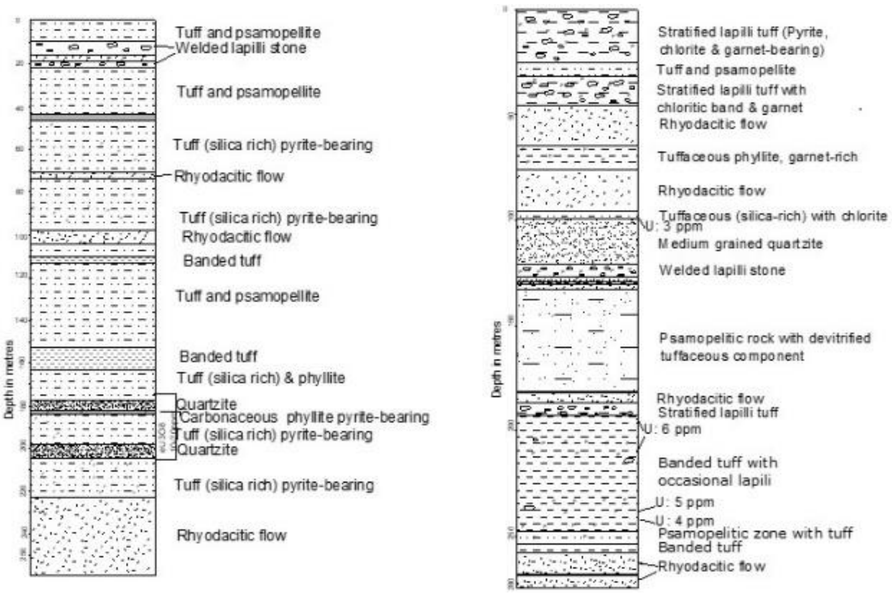

Fig. 12 Left: Litholog of borehole at point A of Fig. 2; Right: Litholog of borehole at point B of Fig. 2. Both show interlayered volcanics and volcaniclastic sequence.

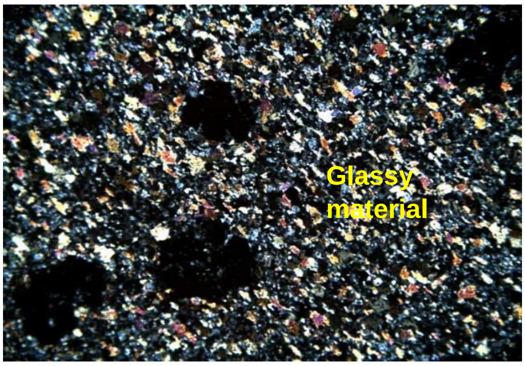

Fig. 13 Clots of glassy material within rhyolite (quartz, sericite and biotite)

Spherulitic structures are quite prominently developed within the lapilli bearing tuffs and tuffaceous sediments depending upon the composition of the parent rocks. The matrix part is composed of tuffaceous as well as non-volcanic components like carbonaceous matter, quartz, biotite and sericite. Radial growth of tremolite and garnet are observed within the recrystallised tuffaceous and pelitic matrix (Fig. 14, 16 and 17). These are later aligned along the schistosity of quartz and sericite grains, which define the regional foliation. Quartz tourmaline veins also traverse through the matrix containing carbonaceous matter and quartzite lapilli containing muscovite (Fig. 18). Chlorite also forms a minor part of the matrix at places. It occurs as an alteration product of garnet and biotite as well. Infiltrations of carbonate materials as veins are also noticed occasionally within the matrix part.

Meramec allanite and zircon have been observed in the volcaniclastics and volcanics by petrological studies (Fig. 19 and 20). Pleochroic haloes are observed in the biotite due to the presence of inclusions of metamict allanite (Fig. 21).

Petrography

The felsic and intermediate flows are mainly composed of quartz, biotite, sericite and feldspar. Feldspars are altered to sericite invariably. Clots of glassy matters are often observed in these rocks (Fig. 13). Lapillis within the volcaniclastics are mostly identified as quartzite, consisting of quartz grains entirely (Fig. 14). These are commonly seen scattered in the tuffaceous horizon as observed in borehole cores. In some tuffaceous rocks, lapillis are constituted of fine to medium grained quartz and some sericite indicating rhyolitic composition (Fig. 15).

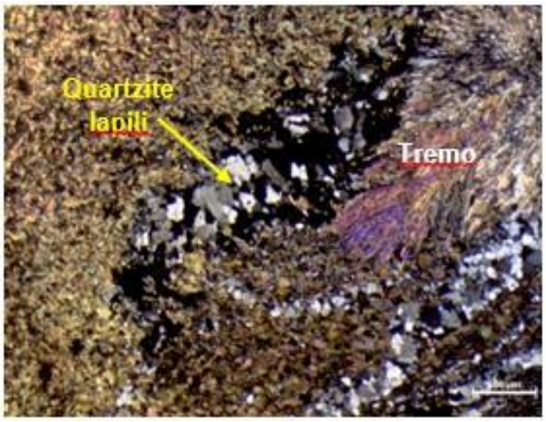

Fig. 14 Quartzite lapilli and spherulitic tremolite with quartz veining

Fig. 15 Rhyolitic lapilli (RL) within tuffaceous matter

Table 4: Intrinsic U and Th content in felsic volcanics and volcaniclastics of Kharidih-Bareda area (Radiometric Assay)

Rock type	eU_3O_8 ppm	Ra eU_3O_8 ppm	ThO_2 ppm	Th/U
Tuffaceous rocks (n=42)	<2 - 35	<5 - 7	<10 - 40	2.7 – 11.2
Felsic volcanic (n=25)	2 – 38	<5 -9	<10 – 48	3.2-13.2
Carbonaceous Phyllite (n=12)	13 - 28	<5 - 10	<10 - 21	1.7-8.4

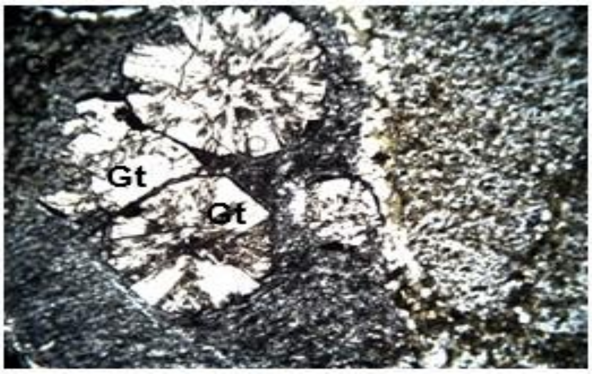

Fig. 16 Spherulitic garnet (Gt) in tuffaceous and argillaceous matrix

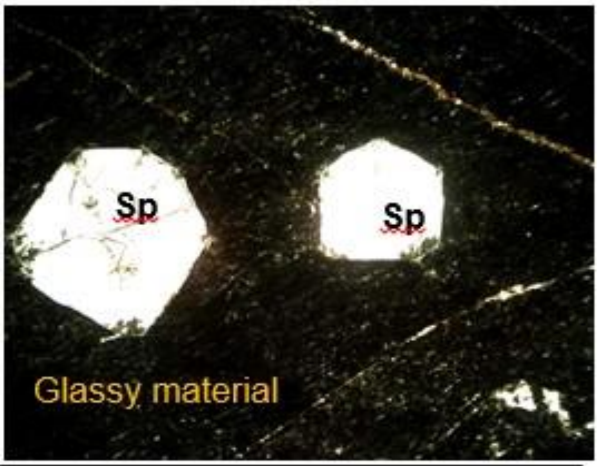

Fig. 17 Spherulitic matter (Sp) in glassy material

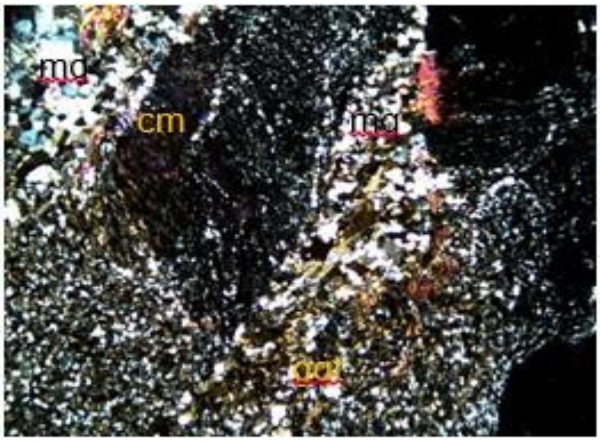

Fig. 18 Carbonaceous matter (cm) garnet quartz tourmaline (gqt) band with muscovite quartzite (mq)

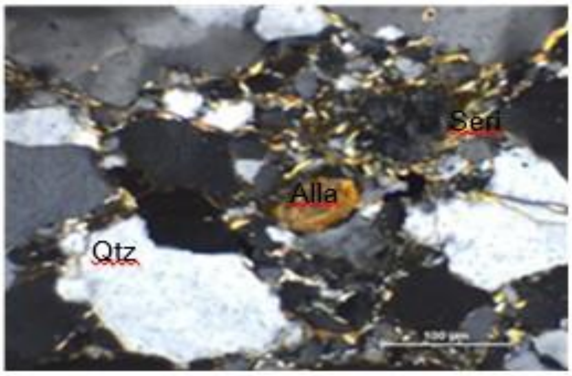

Fig. 19 Metamict allanite (Alla) in quartz-sericite rich rock

Geochemistry

Geochemical analysis of the borehole core samples of volcaniclastics and volcanic rocks were carried out by Wavelength Dispersive X-ray

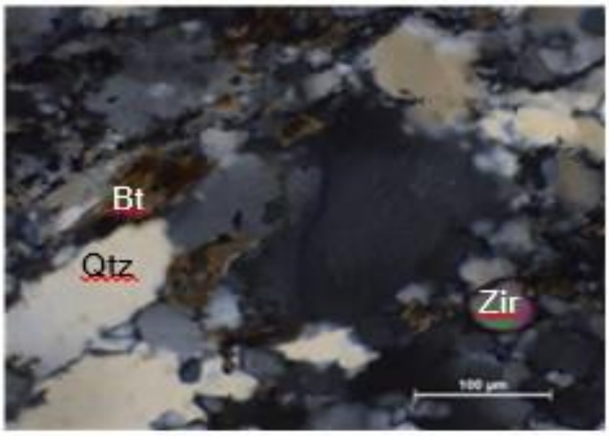

Fig. 20 Metamict zircon (Zir) in quartz and biotite-rich metasediments

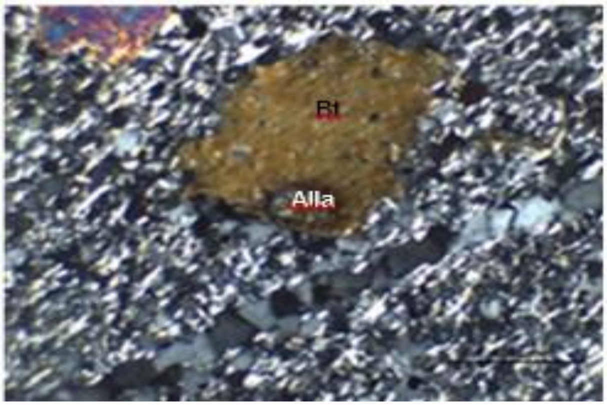

Fig. 21 Pleochroic halo in biotite due to allanite seen in sericite-biotite-quartz-rich rhyolitic rock. Quartz vein is also seen

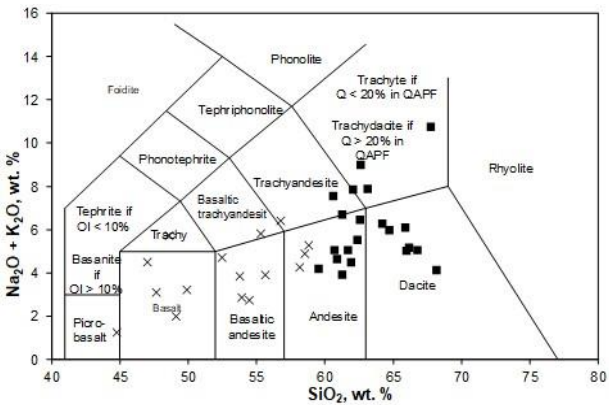

Fig. 22 Total alkali silica plot after Le Bas et al. (1986). From Fig. 22 to Fig. 26 samples of volcaniclastics and felsic volcanics are represented by cross symbols and solid squares, respectively.

fluorescence (WDXRF) at the XRF Laboratory of Atomic Minerals Directorate for Exploration and Research, Nagpur. Felsic volcanic flows have analysed SiO_2: 59.57-68.20%, TiO_2: 0.45-1.22%, Al_2O_3: 8.03-15.92%, Fe_2O_3(t): 7.31-19.55%, MgO: 2.6-3.79%, CaO: 0.38-4.13%, Na_2O: 0.03-2.72%, K_2O: 3.59-6.12% and P_2O_5: 0.05-0.22% (Table 2). The volcaniclastics show wide variation in major elemental concentration viz., SiO_2: 44.81-67.79%, TiO_2: 0.18-0.71%,, Al_2O_3: 0.88-11.93%, Fe_2O_3(t): 6.98-31.57%, MgO: 2.18-5.14%, CaO: 0.71-6.63%,

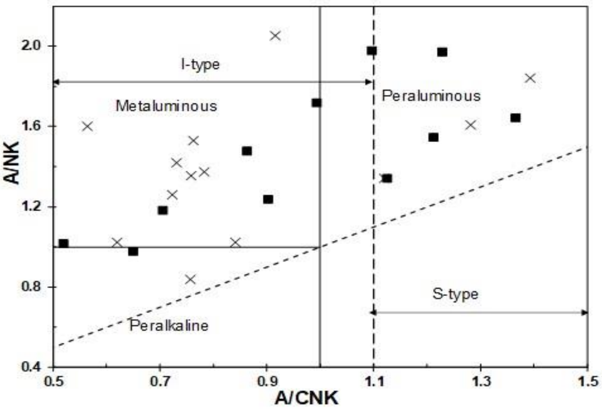

Fig. 23 A/CNK and A/NK plot after Maniar and Picoli (1989)

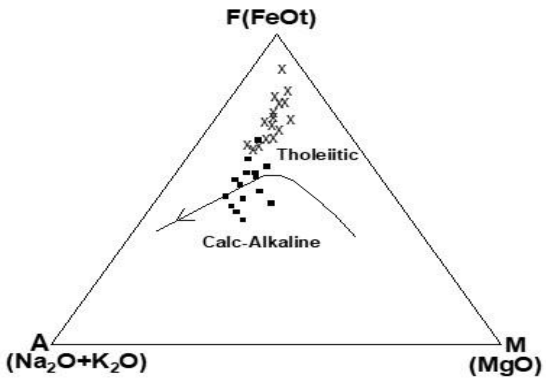

Fig. 24 AFM plot after Irvine and Barangar (1971)

Na_2O: 0.03-3.49% and K_2O: 0.39-7.47%, P_2O_5: 0.08-1.36% (Table 3).

On total alkali vs silica plot of Le Bas et al. (1986) the felsic volcanics mostly fall in andesite-dacite field whereas the volcaniclastics straddle across basalt to basaltic andesite field (Fig. 22). A/CNK and A/NK plot (Maniar and Picoli, 1989) indicate the spread of felsic volcanics from metaluminous to peraluminous compositional range (Fig. 23). But the volcaniclastics fall in meta-aluminous field. This is also corroborated mineralogically by the occurrence of both hornblende and garnet associated with the rock suites. Similar

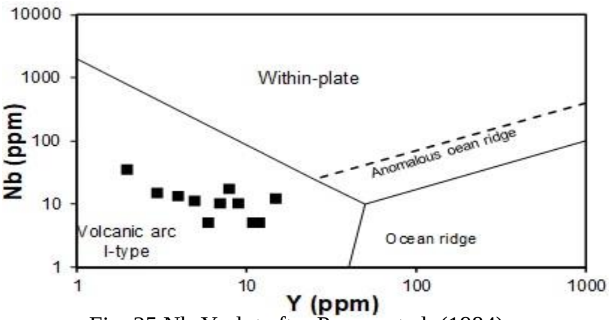

Fig. 25 Nb-Y plot after Pearce et al. (1984)

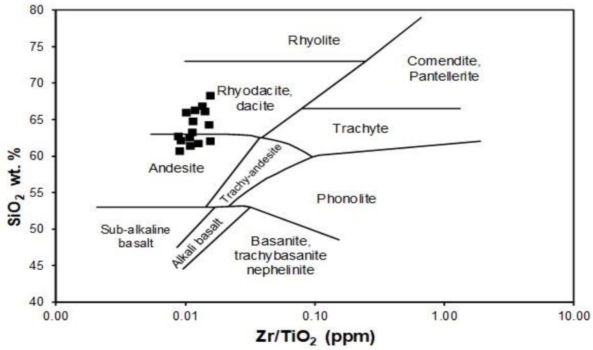

Fig. 26 Zr/TiO_2 vs SiO_2 plot after Winchester and Floyd (1977)

observation showing clear separation of both the suites of lithotypes is also indicated by AFM plot (Irvine and Barangar, 1971) (Fig. 24). In felsic volcanic, Ba content varies from 479 ppm to 1585 ppm, Zr 52 ppm to 191 ppm, Ce 84 ppm to 245 ppm. Nb vs Y plot (Pearce et al., 1984) shows volcanic arc signature of the rocks (Fig. 25). Zr/TiO_2 vs SiO_2 (Winchester and Floyd, 1977) plot of the felsic volcanic suggests that the samples clustered around andesite to rhyodacite-dacite field (Fig. 26).

Suitability of Chandil Formation as prospective uranium source rock

Felsic volcanic and volcaniclastics have radiometrically assayed intrinsic uranium content ranging <5- 7 ppm (n=42) and <5-9 ppm (n=25) respectively (Table 4). Thorium content in felsic volcanic and volcaniclastics rocks vary from <10 ppm to 40 ppm and <10 ppm to 48 ppm. Elevated intrinsic uranium concentration in these rocks is indicative of good source rock characteristics for uranium mineralization. Metamict allanite and zircon are indicative of the presence of labile uranium in source rocks which can easily contribute uranium into the system (Cuney, 2014). Another important fertile source rock for uranium is carbonaceous phyllite in which high intrinsic uranium content up to 10 ppm (n=12) have been analyzed radiometrically. Gamma ray (ppm) logging of the boreholes drilled in the area indicated intrinsic radioactivity (eU_3O_8) of 10 - 53 ppm, mostly between 10-20 ppm. Therefore, the volcanic-volcaniclastic-argillite litho-assemblage represents a prospective source for uranium.

Discussion and Conclusion

The presence of felsic volcaniclastic rocks in Chandil Formation, preponderantly tuffaceous phyllite, was reported earlier along the SPSZ by Acharya et. al. (2006). However, Kharidih-Bareda area, located about 15 km further south of SPSZ, exposes a variety of volcaniclastic rocks as well as felsic flows indicating that the middle part of Chandil Formation was the prime horizon for felsic volcanism. Earlier researchers argued for fluvial origin of the lower part of Chandil Formation on the basis of compositional and textural immaturity along with lenticular geometry and unimodal orientation of cross-strata of certain patches of sandstones (Mazumder, 2005; Chaterjee et al., 2013; De et al., 2016). However, detailed geological mapping in this key sector indicated sheet-like fine to medium grained quartzite bodies extending up to a kilometer co-folded with volcaniclastics and meta-argillites. The occurrence of interlayers of carbonaceous slate/phyllite and profuse syngenetic pyrite-bearing zones within lapilli-rich volcaniclastics suggests euxenic depositional condition. Concealed horizons of limestone and calcareous formations in association with carbonaceous and pyrite-bearing horizons intercepted in boreholes corroborate marine shelf depositional condition. Lava flow, pyroclastic fall, ash fall deposits suggest effusive activity with an intermittent mild explosion. Thus, three modes of transport viz, flow, traction and suspension are decipherable from the lithotypes and structures of the felsic volcanic rocks.

Geochemistry of volcaniclastics and volcanics of Chandil Formation in Kharidih-Bareda sector shows that the volcaniclastic rocks have a wide variation in silica content (44.81-67.79%) as compared to felsic volcanics (59.57-68.20%). Higher $Fe_2O_{3(T)}$ content (6.98-31.57%) recorded in volcaniclastics is attributed to the profuse presence of pyrite as compared to the volcanic flows (7.31-19.55%). Both syngenetic pyrite, encircling the grain boundaries of lapilli clasts and bedding planes and epigenetic pyrite occupying the fracture and foliation planes are discernible. Major element geochemistry indicates rhyodacitic - andesitic and peraluminous to meta aluminous nature of the volcanics and volcaniclastics. Although there are differences in the geochemical signatures of both felsic volcanics and volcaniclastics, their spatial closeness suggests that these rocks might have been genetically related. Geochemical signatures of HFS elements like Nb, Zr, Y indicate arc-related magmatism of the felsic volcanics.

Granites and rhyolites are considered as primary uranium sources for the formation of uranium deposits. Large uranium deposits such as Streltsovka, Russia, Dornod complex, Mongolia and Olympic Dam, Australia are associated with acidic volcanic and plutonic complexes (Cuney, 2009). Studies by Cuney (2014) have highlighted four types of felsic magmatics, viz, peralkaline, high-K metaluminous calc-alkaline, L-type peraluminous and anatectic pegmatoids, which can be sufficiently enriched in U to represent a significant source for the genesis of U deposits. The presence of uraninite or U in the glassy matrix of the volcanic equivalent of these rock types offers the best possible source. When uranium-bearing accessory minerals are available in metamict state, the high-K calc-alkaline plutonic rocks also becomes a promising U source (Leroy and George-Aniel, 1992; Cuney, 2009). Hydrothermal fluids passing through these minerals can scavenge uranium and carry them to suitable reduction traps. Studies also emphasize the capacity of highly saline, very acidic high temperature oxidizing solution to release uranium even from refractory minerals (Cuney and Mathieu, 2000). Nevertheless, acid volcanics like rhyolite, welded tuff and ignimbrites which contain readily leachable uranium present in the glassy matrix are considered to be ideal sources (Maithani and Srinivasan, 2011).

The Chandil Formation of NSMB is replete with felsic eruptives and effusive components. Based on elevated uranium concentration (up to 9 ppm) in the felsic volcaniclastics and carbonaceous metapelites, a potentially economic source of uranium for volcanic-related hydrothermal uranium deposits is envisaged in the basin. The presence of metamict allanite and zircon, and pleochroic haloes in the peraluminous to metaluminous felsic volcanics and volcaniclastics supports source rock favourability for uranium. Anomalous zones of uranium mineralization showing polymetallic signature (U-Cu-Au-Ag-REE), hosted by ferrugenised brecciated carbonaceous and cherty phyllite, has been reported at Kantaldih area, at the southern contact of Chandil Formation with Dalma Volcanics (Mishra et al., 1999; Mishra, 2002). Evidence of uranium mineralization in carbonatite-alkali ultramafite environment has been reported from the SPSZ at the northern contact of Chandil Formation with CGGC (Singh, 1977; Katti et al., 2010). Hence, based on such signatures of mineralisation, efficient remobilization of uranium by hydrothermal fluids is envisaged within Chandil Formation Thermal effect for such mobilization can be imparted by felsic and basic intrusives. Structural conduits like concealed shear and fracture zones sympathetic to Dalma thrust and SPSZ would provide passage for movement of uranium bearing fluid. Intercalatory bands of carbonaceous metapelite, ferruginous material and pyrite-bearing horizons can form reduction zones along suitable structural traps. Thus, the study suggests that Chandil Formation represents an environment wherein suitable provenance and host rock for uranium mineralization exists within the same geological domain, which necessitates further research.

Acknowledgement

The authors are thankful to Director, Atomic Minerals Directorate for Exploration & Research (AMD) for permitting to publish the paper. Encouragement provided by Additional Director (Op-I) is thankfully acknowledged. Thanks are due to the scientists of different laboratories for providing analytical support.

References

Acharya, A., Ray, S., Choudhuri, B.K., Basu, S.K., Bhadhuri, S.K. and Sanyal, A.K. (2006), Proterozoic rock suites along South Purulia Shear Zone, Eastern India: Evidence for rift – related setting: Jour. Geol. Soc. Ind, v. 68, p. 1069-1086.

Chatterjee, P., De, S., Ranaivoson, M., Mazumder, R and Arima, M (2013), A review of the ~1600 Ma sedimentation, volcanism, and tectono-thermal events in the Singhbhum craton, Eastern India: Geosci. Front., v. 4 (3), p. 277-287.

Cuney, M. and Mathieu, R. (2000), Extreme light rare earth element mobilization by diagenetic fluids in the geological environment of the Oklo natural reactor zones, Franceville basin, Gabon: Geology, v. 28, p. 743-746.

Cuney, M. (2009), The extreme diversity of uranium deposits: Miner. Dep. v. 44, p. 3-9.

Cuney, M. (2014), Felsic magmatism and uranium deposits: Bulletin de la Societe Geologiquue de France, v. 185 (2), p. 75-92.

De, S., Mallik, L., Mazumder, R., Chatterjee, P., Ohta, T., Saito, S. and Chiarenzelli, J. (2016), Sedimentation history of the Paleoproterozoic Singhbhum Group of rocks, Eastern India and its implications: Earth-Science Reviews, v. 163, p. 141-161.

Dunn, J.A. and Dey, A.K., (1942), Geology and petrology of Eastern Singhbhum and surrounding areas: Geol. Surv. Ind. Mem., v. 69 (2), p. 281-456.

Fisher, R. V. (1966), Rocks composed of volcanic fragments: Earth Science Review, v. 1, p. 287–298.

Gupta, A and Basu, A. (2000), North Singhbhum Proterozoic Mobile Belt, Eastern India- a review: Geol.Surv. Ind. Spl. Pub.,v. 55, p. 195-226.

Irvine, T.N. and Barangar, W.R.A. (1971), A guide to the chemical classification of the common volcanic rocks: Canadian Jour. of Earth Sci., v. 8, p. 523-548.

Katti, V.J., Sen,Joydip and Bhatt, A. K. (2010), Uranium potentiality of South Purulia Shear Zone. Paper presented in Technical committee meeting on low grade uranium deposits at IAEA, Vinnea, March 29-31.

Le Bas, M.J., Le Maitre, R.W., Streckeisen, A. and Zanettin, B. (1986), A chemical classification of volcanic rocks based on the total alkali-silica diagram: Journal of Petrology, v. 27, p. 745-750.

Leroy J. and George-Aniel B. (1992), Volcanism and uranium mineralisations: the concept of source rock and concentration mechanism: J. Volcan. Geotherm. Res, v. 50, p. 247-272.

Mahadevan, T. M. (2002), Geology of Bihar and Jharkhand: Geol. Soc. Ind., 563pp.

Maithani, P.B. and Srinivasan, S. (2011), Felsic volcanic rocks, a potential source of uranium - An Indian Overview: Energy Procedia, v. 7, p. 163–168.

Maniar, P.D. and Piccoli, P.M. (1989), Tectonic discrimination of granitoids: Geol. Soc. Am., v. 101, p. 635-643.

Mazumdar, R. (2005), Proterozoic sedimentation and volcanism in the Singhbhum crustal province, India and their implications: Sed. Geol., v. 176, p. 167-193.

Mazumder, R., De, S., Ohta, T.,D. Flannery, Mallik, L., C haudhury, T.,Chatterjee, P., Ranaivoson, M.A. and Arima,M. (2015), Palaeo-Mesoproterozoic sedimentation and tectonics of the Singhbhum Craton, Eastern India, and implications for global and craton-specific geological events: Geol. Soc. Lond., v. 43 (1), p. 139-149.

Mishra, K.S., Gupta, K.R., Bagchi, A.K. and Singh, Jagmer (1999), Proterozoic Iron Oxide (Cu-Ni-U-REE) type mineralization in the environs of Dalma Volcanics, West Singhbhum District, Bihar, A new horizon for exploration for polymetallic ores: Jour. Geol. Soc. Ind., v. 54, p. 491-494.

Mishra, K.S. (2002), Geochemistry of Proterozoic carbonaceous metasedimentaries from the northern part of Dalma metavolcanics belt, West Singhbhum district, Jharkhand: Implications for its provenance: Jour. of Applied Geochemistry, v. 4(2), p. 212-227.

Pearce, J.A., Harris, N.W. and Tindle, A.G. (1984), Trace element discrimination diagrams for the tectonic interpretation of granitic rocks: Journal of Petrology. v. 25, p. 956-983.

Ray, K. K., Ghosh Roy, A. K. and Sengupta, S. (1996), Acid volcanic rocks between the Dalma volcanic belt and the Chhotanagpur Gneissic Complex, East Singhbhum and Purulia Districts of Bihar and West Bengal: Ind. Mineral., v. 50, p. 956-983.

Reddy, S. M., Clarke, C. and Mazumder, R., (2009), Temporal constraints on the evolution of the Singhbhum Crustal Province from U-Pb SHRIMP data. In Saha, D.,Mazumder, R., (Eds.), Paleo-proterozoic Super Continents and Global Evolution: International Association for Gondwana Research Conference Series, Abstract v. 9, p. 17-18.

Sengupta, S., Sarkar, G., Ghosh-Roy, A. K., Bhaduri, S. K., Gupta, S. N. and Mandal, A. (2000), Geochemistry and Rb-Sr Geochronology of acid tuffs from the northern fringe of the Singhbhum craton and their significance in the Precambrian evolution: Ind. Miner., v. 54, p. 43-56.

Singh, G (1977), Status of exploration for atomic minerals in Purulia district, West Bengal and future possibilities, In: Sem. Vol. Mineral resources and mineral-based industries in Purulia district, W. B- Prospects and perspectives: Mines, Metals and Fuels. Special Publn. p. 61-65.

Winchester, J.A. and Floyd, P.A. (1977), Geochemical discrimination of different magma series and their differentiation products using immobile elements: Chem. Geol., v. 20, p. 325-343.

Received: 12th July, 2020
Revised Accepted: 13th August, 2021